Journal of Integrative Agriculture 2026, 25(7): 3044–3057

Available online at ScienceDirect

Journal of Integrative Agriculture

RESEARCH ARTICLE

Convergent dynamics and shared mechanisms of three-pool soil carbon mineralization under different grassland managements

Junhao Feng[1*], Ji Chen[2*], Xiaowei Liu[3], Yudu Jing[4, 5, 6], Ke Liang[3], Qiang Yu[5, 7], Changhui Peng[8, 9], Liang Guo[7, 10, 11#]

[1] *State Key Laboratory of Soil and Water Conservation and Desertification Control, College of Soil and Water Conservation Science and Engineering, Northwest A&F University, Yangling 712100, China*
[2] *State Key Laboratory of Loess and Quaternary Geology, Institute of Earth Environment, Chinese Academy of Sciences, Xi'an 710061, China*
[3] *College of Grassland Agriculture, Northwest A&F University, Yangling 712100, China*
[4] *The Research Center for Soil and Water Conservation and Ecological Environment, Chinese Academy of Sciences and Ministry of Education, Yangling 712100, China*
[5] *Institute of Soil and Water Conservation, Chinese Academy of Sciences and Ministry of Water Resources, Yangling 712100, China*
[6] *University of Chinese Academy of Sciences, Beijing 100049, China*
[7] *State Key Laboratory of Soil and Water Conservation and Desertification Control, Northwest A&F University, Yangling 712100, China*
[8] *School of Geographic Sciences, Hunan Normal University, Changsha 410081, China*
[9] *Department of Biology Science, Institute of Environment Sciences, University of Quebec at Montreal, Montreal H3C3P8, Canada*
[10] *Key Laboratory of the Alpine Grassland Ecology in the Three Rivers Region (Qinghai University), Ministry of Education, Xining 810016, China*
[11] *Administration Bureau of Ningxia Yunwushan National Nature Reserve, Guyuan 756000, China*

Highlights

- A three-pool model coupled with 553-day incubation reveals carbon pool decomposition.
- Mineralization shifts from active to passive pools in enclosed and grazed soils.
- Similar mineralization mechanisms are shared, despite faster rates in enclosed soils.
- Microbial strategies and enzyme activities jointly regulate SOC mineralization.

Abstract

The mineralization dynamics of soil organic carbon (SOC) in grasslands are crucial to terrestrial biogeochemical cycles. However, the regulatory mechanisms underlying extracellular enzyme metabolism and microbial community structure during SOC mineralization across different carbon pools remain poorly understood. In this study, a 553-day incubation experiment was conducted to examine temporal changes in CO_2 emissions, extracellular enzyme activities, microbial biomass, and microbial community composition in soils from both enclosed and grazed grasslands. Using a three-pool model, SOC dynamics were quantified within active, slow, and passive carbon pools, revealing a shift in the dominance of mineralization from the active carbon pool to the passive carbon pool during the long-term carbon turnover, with differences observed across grassland management strategies. Compared to grazed grasslands, enclosed grasslands exhibited an approximately 110% larger active carbon pool and higher initial SOC mineralization rates (significantly higher during the first 113 days), yet long-term microbial and enzymatic regulatory mechanisms — particularly shifts in microbial strategies, enzyme activity patterns, and their interactions with carbon pools — were similar across both management regimes. The observed shifts in carbon pool dynamics were driven by enhanced microbial capacity to decompose passive carbon, associated with substantially increased oxidative enzyme production (e.g., mass-specific oxidase activity increased by 190.6% in enclosed soil and by 256.1% in grazed soil) and elevated nitrogen and phosphorus demands. Notably, microbial communities shifted from fast-growing copiotrophic taxa (e.g., Proteobacteria, Bacteroidetes, Ascomycota) to slower-growing oligotrophic taxa (e.g., Acidobacteria, Actinobacteria, Planctomycetes, Basidiomycota), with the oligotroph-to-copiotroph ratio increasing by 55.5–62.6% for bacteria and 96.9–247.5% for fungi. These changes were closely linked to shifts in enzyme activity profiles and stoichiometric ratios. Overall, this study provides mechanistic insights into how microbial ecological strategies and enzyme activities interact to regulate SOC mineralization across different pools under contrasting grassland management

Received 12 May 2025; Received in revised form 12 September 2025; Accepted 30 October 2025; Available online 18 December 2025
[#]Correspondence Liang Guo, Mobile: +86-18709221128, E-mail: guoliang2014@nwafu.edu.cn
[*]These authors contributed equally to this study.

doi: 10.1016/j.jia.2025.12.030

regimes. These findings advance our understanding of SOC turnover and improve predictive capabilities for carbon cycling, with broader implications for global climate change feedbacks.

Keywords: soil organic carbon mineralization, soil respiration, three-pool model, microbial community, extracellular enzyme, incubation experiment, grasslands

1. Introduction

Microbial respiration is a key driver of soil organic carbon (SOC) mineralization and plays a critical role in regulating global carbon cycles and climate feedbacks (Melillo *et al.* 2017). SOC is inherently heterogeneous, comprising various components with distinct turnover times and decomposition potentials, ranging from labile to recalcitrant forms (Trumbore 1997; Zhang *et al.* 2025). The three-pool model, which classifies SOC into active, slow, and passive pools, is widely used to explore SOC mineralization dynamics, integrating data from long-term microbial respiration studies (Liang *et al.* 2015; Guo *et al.* 2020; Schädel *et al.* 2020; Xiang *et al.* 2023). Although the model provides key insights into carbon pool stability and turnover, it lacks integration of critical biochemical and microbial processes, such as extracellular enzyme activities and microbial community shifts. A comprehensive understanding of three-pool dynamics, in combination with the biochemical and microbial drivers of SOC mineralization over long-term periods, is essential for refining model predictions and advancing mechanistic insights into SOC turnover. This, in turn, will improve forecasts of ecosystem carbon cycling under changing conditions.

The mineralization of SOC is governed by a complex interplay of abiotic and biotic factors. Abiotic factors, such as substrate availability, pH, soil texture, and moisture, influence microbial respiration by regulating microbial activity and community composition (Luo and Zhou 2006; Kittredge *et al.* 2016; Hu *et al.* 2025). In contrast, extracellular enzymes are pivotal in SOC mineralization, with enzymatic depolymerization often acting as the primary rate-limiting step (Domínguez *et al.* 2017; Chen *et al.* 2018; Kittredge *et al.* 2018). As SOC mineralization progresses, labile carbon fractions are rapidly consumed, prompting microorganisms to upregulate oxidative enzyme activities to degrade more recalcitrant carbon forms (Kittredge *et al.* 2018; Li *et al.* 2023). While some studies suggest that changes in extracellular enzyme categories and activities regulate the mineralization of distinct carbon pools (Wang J *et al.* 2020b), others argue that no such correlation exists, proposing that SOC mineralization is not constrained by variations in enzyme activity (Birge *et al.* 2015). These discrepancies likely arise from differences in experimental conditions, such as carbon substrate additions and study durations. Therefore, long-term soil incubation experiments are essential for understanding SOC decomposability, as they allow observation of microbial carbon utilization in the absence of new organic inputs (Huo *et al.* 2017; Ma *et al.* 2019). However, the specific roles of enzymes, including oxidases and hydrolases, in SOC turnover, and how their stoichiometry and activities change during incubation remain unclear.

Microorganisms, as primary producers of soil extracellular enzymes, are directly involved in SOC mineralization. Changes in microbial community structure and biomass have significant impacts on soil respiration (Rousk *et al.* 2012; Xiang *et al.* 2024). The rapid depletion of labile carbon fractions during SOC mineralization forces microbial communities to adopt diverse ecological strategies (Delgado-Baquerizo *et al.* 2016). Among them, copiotrophic (r-strategists) microbes thrive in carbon-rich environments, grow rapidly, and promote fast carbon mineralization, whereas oligotrophic (K-strategists) microorganisms grow slowly but are more effective at degrading recalcitrant carbon (Fierer *et al.* 2007; Ho *et al.* 2017). Shifts towards oligotrophic fungi have been linked to reduced CO_2 emissions due to a decrease in overall fungal abundance and increased dominance of oligotrophic species (Qiu *et al.* 2023). Additionally, enzyme production, an essential microbial foraging strategy, is closely linked to microbial community composition (Yang *et al.* 2021; Koranda *et al.* 2023). Understanding the relationship between extracellular enzyme activity and microbial community composition, especially within ecological strategy frameworks, is crucial for assessing microbially mediated turnover of carbon pools (Fierer 2017; Yang *et al.* 2023).

Grasslands, which cover approximately 40.5% of the Earth's land surface (White *et al.* 2000), are essential components of terrestrial ecosystems and play a key role in both regional and global carbon cycles (Bai and Cotrufo 2022; Liu L *et al.* 2023). Enclosure, a widely used management practice for restoring degraded grasslands, is generally believed to enhance soil carbon sequestration (Wang *et al.* 2023; Qu *et al.* 2024). However, studies in alpine meadows on the northeastern Tibetan Plateau showed that enclosure significantly increased soil microbial respiration (Wang J *et al.* 2020a), indicating that the effects of enclosure can vary across ecosystems. Enclosure alters vegetation composition (Xu *et al.* 2015; Liu *et al.* 2025), restructures carbon and nutrient pools (Feyisa *et al.* 2017), shifts soil microbial community (Wu *et al.* 2022; Tang *et al.* 2025), and modifies soil physical and chemical properties (Wang L *et al.* 2020). These changes lead to distinct differences in carbon pool composition and microbial communities between enclosed and grazed grasslands. Investigating the long-term dynamics of SOC mineralization and its driving factors across different grassland management regimes is essential for enhancing our understanding of SOC turnover mechanisms and informing optimized grassland management strategies.

This study employs a long-term (553-day) soil incubation experiment, high-resolution soil respiration measurements, and the three-pool model to examine the long-term

mineralization dynamics of SOC pools and their driving mechanisms in grasslands under contrasting management regimes (enclosure *vs*. grazing). The study aims to: (I) quantify the mineralization dynamics of three distinct SOC pools; (II) elucidate the microbial mechanisms driving SOC pool mineralization under different management practices. We hypothesize that: (I) As incubations progress and the labile C pool is depleted, microorganisms will increase oxidative enzyme production to degrade the recalcitrant carbon pool; (II) microbial communities will shift towards oligotrophic species, reducing the dominance of copiotrophic species; and (III) the mineralization dynamics of SOC pools and the associated microbial mechanisms will converge across different grassland management regimes, despite initial differences in carbon pool composition (Fig. 1).

2. Materials and methods

2.1. Study site

This study was conducted in the Yunwushan National Nature Reserve (36°10′–36°17′N, 106°21′–106°27′E, 1,800–2,100 m a.s.l.) on the Loess Plateau, China, which hosts the region's largest and best-preserved typical grassland. The region has a semiarid climate, with an average annual precipitation of 425 mm, over 60% of which falls between July and September. The mean annual temperature is 7.0°C, with an average minimum of –8.2°C in January and an average maximum of 25.2°C in August. The soil in the area is classified as montane gray-cinnamon soil. The dominant vegetation includes *Stipa bungeana*, *Stipa grandis*, *Thymus mongolicus*, *Artemisia sacrorum*, and *Potentilla acaulis* (Appendix A; Liu X *et al.* 2023).

2.2. Experimental design and soil sampling

In August 2017, soil samples were collected from two sites with contrasting management regimes: one that had been enclosed for 10 years, and the other subjected to continuous grazing at a density of four sheep per hectare. Both sites had similar soil types, elevations, slopes, and aspects (Appendix A). At each site, three plots (50 m×100 m) were established, spaced 80–100 m apart. Soil samples were collected from the top 20 cm of the soil profile using a 5 cm diameter auger, following the removal of surface litter (Fig. 2). Ten soil cores were collected along an S-shaped transect in each plot and combined into one composite sample. The composite samples were sieved to remove roots, stones, and debris, then divided into two subsamples: one air-dried for physicochemical analysis, and the other temporarily stored at 4°C for soil incubation experiments.

The soil incubation experiment proceeded as follows: approximately 500 g of fresh soil was collected from both enclosed and grazed sites and placed in transparent glass bottles (Fig. 2). Soil moisture content was adjusted to 60% of field capacity using distilled water. Six replicates were prepared for each management regime, divided into two groups: one for CO_2 emissions monitoring and the other for soil property analysis (Fig. 2). All samples were incubated at a controlled temperature of 25°C for 553 days (~1.5 years). The extended incubation duration (553 days) was specifically designed to capture, to the greatest extend, the full trajectory of SOC mineralization, including both the rapid depletion of labile carbon and the subsequent turnover of more recalcitrant carbon pools. This approach facilitated a comprehensive investigation of microbial and enzymatic mechanisms extending beyond the initial active carbon

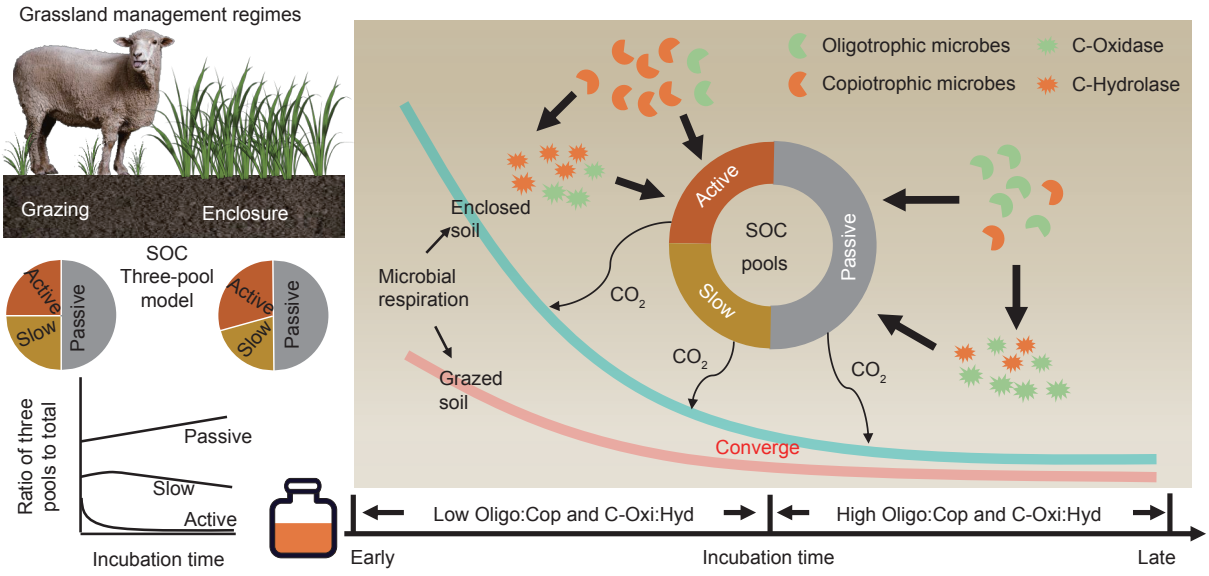

Fig. 1 Conceptual model of microbial and enzyme-mediated soil organic carbon (SOC) dynamics during long-term incubation of enclosed and grazed grassland soils. It is hypothesized that enclosed soils should exhibit higher carbon mineralization rates than grazed soils; however, the key drivers of SOC mineralization dynamics may share similar characteristics across both management regimes. Shifts in microbial ecological strategies, particularly between oligotrophic and copiotrophic species, can influence SOC dynamics either directly or indirectly by affecting the allocation of extracellular enzymes. Oligo:Cop, the ratio of oligotrophic to copiotrophic microorganisms; C-Oxi:Hyd, the ratio of carbon oxidase to carbon hydrolase activities.

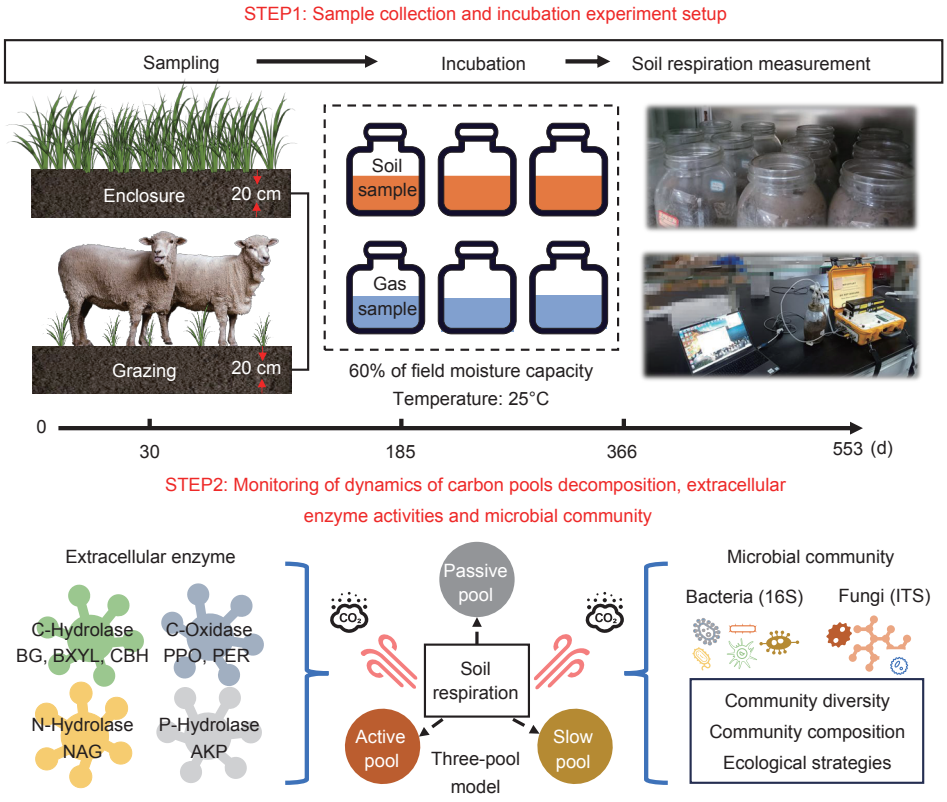

Fig. 2 Sampling and experimental design in this study. BG, β-1,4-glucosidase; BXYL, β-1,4-xylosidase; CBH, β-D-cellulosic biohydrolase; PPO, polyphenol oxidase; PER, peroxidase; NAG, β-1,4-N-acetyl-glucosaminidase; AKP, alkaline phosphatase; Ecological strategies, copiotrophs *vs*. oligotrophs (r-strategists *vs*. K-strategists).

phase. In the CO_2 emissions monitoring group, microbial respiration rates were recorded daily during the first 14 days using an automated soil carbon flux measurement system (LI-8100, LI-COR, Inc., Lincoln, NE, USA). Thereafter, measurements were taken every 3 days until day 150, and then biweekly until the end of the incubation period (day 553). Soil moisture was regularly adjusted using the gravimetric method throughout the experiment. Meanwhile, samples from the soil property analysis group were collected at predefined intervals to assess microbial biomass carbon (MBC), soil enzyme activities, and soil microbial community composition. These intervals occurred at 30 days (one month), 185 days (0.5 year), 366 days (1 year), and 553 days (end of the incubation period) (Fig. 2).

2.3. Soil respiration model — Three-pool model

Model description We used a modified first-order kinetic model, adapted from Andren and Paustian (1987), to partition observed CO_2 emissions into active (A_1C), slow (A_2C), and passive (A_3C) SOC pools. The model is expressed by the following equations (Liang *et al.* 2015; Guo *et al.* 2017):

$$R_{cum}=\sum_{i=1}^{3}A_iC_{tot}(1-e^{-k_it}) \quad (1)$$

$$A_i=C_i/C_{tot} \quad (2)$$

$$R_i=C_ik_ie^{-k_it} \quad (3)$$

$$P_i=C_ie^{-k_it} \quad (4)$$

where R_{cum} (mg C g^{-1} soil) represents cumulative carbon mineralization after incubation time t. A_i (i=1, 2, 3), the partitioning coefficient, denotes the initial fractions of the active, slow, and passive SOC pools, respectively, subject to the constraint $A_1+A_2+A_3=1$. C_{tot} (mg C g^{-1} soil) represents the initial SOC content. k_i (d^{-1}) is the decay rate constant for the ith pool. C_i (mg C g^{-1} soil) indicates the initial content of each carbon pool. R_i (mg C g^{-1} soil d^{-1}) represents soil respiration rate from each SOC pool after incubation time t. P_i (mg C g^{-1} soil) reflects the remaining content of each carbon pool after incubation time t. The key parameters estimated in this study were the partitioning coefficients (A_i) and the carbon decay rates (k_i).

Data assimilation We applied a Bayesian probabilistic inversion approach (Xu *et al.* 2006) to estimate the model parameters A and k:

$$p(\theta|Z) \propto p(Z|\theta)p(\theta) \quad (5)$$

The posterior probability density function (PDF) of the parameters θ, denoted as $p(\theta|Z)$, can be derived from prior knowledge of the parameters, represented by the prior PDF — $p(\theta)$, and the information contained in the soil incubation data, represented by the likelihood function $p(Z|\theta)$. The likelihood function $(Z|\theta)$ was calculated under the assumption that the errors between observed and modeled values are independent, with a multivariate Gaussian distribution and a mean of zero:

$$p(Z|\theta) \propto \exp\left\{-\sum_{i=1}^{3}\sum_{t\in obs(Z_i)}\frac{[Z_i(t)-X_i(t)]^2}{2\sigma_i^2(t)}\right\} \quad (6)$$

where $Z_i(t)$ and $X_i(t)$ represent the observed and modeled cumulative respiration values, respectively, and $\sigma_i(t)$ is the

standard deviation of observations. We used the Metropolis-Hastings (M-H) algorithm to generate posterior PDFs of parameters (Metropolis *et al.* 1953; Hastings 1970). The M-H algorithm involves two repeating steps: the proposing step and the moving step (Xu *et al.* 2006). In each proposal step, the algorithm generates a new parameter θ^{new} on the basis of the previously accepted parameter θ^{old} with a proposal distribution $p(\theta^{new}|\theta^{old})$:

$$\theta^{new}=\theta^{old}+r(\theta_{max}-\theta_{min})/D \quad (7)$$

where θ_{max} and θ_{min} are the upper and lower bounds of the prior range for the given parameter; r is a random variable between –0.5 and 0.5 with a uniform distribution, and D controls the proposing step size and was set to 10 in this study (Liang *et al.* 2015). In the moving step, the algorithm determines whether θ_{new} should be accepted or rejected. Data from the long-term laboratory incubation experiment (R_{cum}), combined with the SOC mineralization multi-pool model, were used to optimize the model parameters (A_i and k_i). The Gelman-Rubin diagnostic was employed to check parameter convergence and ensure the stability of posterior distributions (Gelman and Rubin 1992).

2.4. Analysis of soil properties and enzyme activities

This study assessed key soil properties, including soil organic carbon (SOC), nitrogen and phosphorus-related variables, soil pH and moisture, microbial biomass carbon (MBC), and enzyme activities. SOC was determined using dichromate oxidation, and total nitrogen was measured using an automatic Kjeldahl analyzer (Kjeltec 8400, FOSS Corporation, Denmark). Available phosphorus was determined using the Olsen method, while ammonium nitrogen and nitrate nitrogen were assessed using a continuous-flow auto-analyzer (Alpkem, OI Analytical, USA). Soil pH was determined in a 1:2.5 soil-to-water suspension, and soil moisture content was measured by oven-drying method. For detailed procedures, refer to Liu X *et al.* (2023). MBC was analyzed *via* fumigation extraction (Vance *et al.* 1987). Extracellular enzyme activities essential for C, N, and P cycling were also evaluated. Specifically, activities of two key oxidases — polyphenol oxidase (PPO) and peroxidase (PER) — which degrade recalcitrant carbon — were measured. The activities of three hydrolases involved in C metabolism — β-1,4-glucosidase (BG), β-1,4-xylosidase (BXYL), and β-D-cellulosic biohydrolase (CBH), which break down labile carbon compounds, were quantified. Furthermore, two hydrolases related to N and P metabolism — β-1,4-N-acetyl-glucosaminidase (NAG) and alkaline phosphatase (AKP) — were evaluated. Hydrolase activities (BG, BXYL, CBH, AKP, and NAG) were quantified using a fluorescence microplate assay with 4-methylumbelliferone (MUB) linked model substrates (Marx *et al.* 2001). Briefly, fresh soil (1 g) was mixed with 125 mL deionized water, agitated at 25°C for 2 h, and 1 mL of the suspension was incubated with 250 µL substrate solution at 25°C for 4 h in the dark. The reaction was stopped with 50 µL NaOH, and 250 µL of the mixture was transferred to a black 96-well plate for fluorescence reading (excitation: 365 nm, emission: 450 nm) using a microplate reader (SpectraMax M2, Molecular Devices, USA). Controls included negative, blank, quench, and reference standard. The results were expressed in units of nmol substrate converted per mL of sample, with units of nmol h^{-1} g^{-1}. Six replicate wells were tested for each sample. Oxidase activities (PPO and PER) were measured spectrophotometrically using L-3,4-dihydroxy-phenylalanine as the substrate (German *et al.* 2011), and absorbance was measured at 450 nm. The unit of enzyme activity was expressed as the rate of catalytic reaction, i.e., milligrams of substrate transformed per gram of dry soil per hour. All measured activities significantly exceeded the background blank values, therefore ensuring the robustness of the quantification process. Cumulative activity of C-related hydrolase (C-Hydrolase) was calculated as the sum of BG, BXYL, and CBH activities, while C-related oxidase (C-Oxidase) activity was the sum of PPO and PER activities. The ratio of C-Oxidase to C-Hydrolase was used to evaluate the balance between oxidative and hydrolytic processes in carbon metabolism, indicating the relative importance of recalcitrant versus labile carbon decomposition (Li *et al.* 2018; Chen *et al.* 2020). Additionally, mass-specific enzyme activity normalized to MBC was used to assess enzyme efficiency relative to changes in enzyme production and degradation (Steinweg *et al.* 2013; Yu *et al.* 2019).

2.5. Composition of microbial communities and classification of oligotrophic and copiotrophic species

DNA was extracted from 0.5 g of soil samples using the FastDNA Spin Kit (MP Biomedicals, Cleveland, USA). DNA quality was assessed *via* 1% agarose gel electrophoresis, and quantity was measured using a spectrophotometer (ND1000, NanoDrop Technologies, Wilmington, USA). The V4–V5 region of the bacterial 16S rRNA gene was amplified by PCR using primers 515F (5′-GTGCCAGCMGCCGCGG TAA-3′) and 907R (5′-CCGTCAATTCCTTTGAGT TT-3′). The ITS1 region was amplified for fungal analysis using primers ITS5-1737F (5′-GGAAGTAAAAGTCGTAACAAGG-3′) and ITS2-2043R (5′-GCTGCGT TCTTCATCGATGC-3′). The PCR conditions included an initial denaturation at 98°C for 60 s, followed by 30 cycles of 98°C for 10 s, 50°C for 30 s, and 72°C for 30 s, and a final extension at 72°C for 5 min. PCR products were pooled, purified with a Qiagen Gel Extraction Kit (Qiagen Co., Ltd., Germany), and sequenced on the Illumina MiSeq PE300 platform (Illumina Corporation, San Diego, USA). The average sequencing depths for the 16S and ITS were 17,123 and 81,071 reads per sample, respectively. Sequencing data were analyzed using the EasyAmplicon pipeline (Guo *et al.* 2023). The bacterial oligotroph-to-copiotroph ratio was calculated based on the relative abundances of oligotrophic taxa (e.g., Acidobacteria, Actinobacteria, Planctomycetes*;* Li *et al.* 2021) and copiotrophic taxa (e.g., proteobacteria, Bacteroidetes*;* Fierer *et al.* 2007). The fungal oligotroph-to-copiotroph ratio was calculated from the relative abundances of Basidiomycota (oligotrophs) and Ascomycota (copiotrophs), representing typical fungal ecological strategies (Li *et al.* 2023).

2.6. Statistical analysis

We used MATLAB 2023a for data assimilation of cumulative carbon emissions, where SOC was partitioned into three distinct carbon pools. Estimated parameters included *A*

(carbon pool partitioning coefficient), *k* (carbon decay rate), fR (fraction of each carbon pool's respiration to total respiration, representing the contribution of different carbon pools to overall carbon mineralization), and fP (fraction of each carbon pool to total carbon).

Repeated measures ANOVA was used to assess the effects of different management regimes, incubation duration, and their interaction on soil properties, including extracellular enzyme activities, microbial biomass, and microbial diversity, after testing the normality of the data. Post-hoc pairwise comparisons with the least significant difference (LSD) test were used to evaluate significant differences among treatments. Principal coordinates analysis (PCoA) was employed to visualize variations in bacterial and fungal community structures across treatments. Non-parametric multivariate analysis of variance (Adonis) was applied using the vegan package to statistically assess differences in microbial communities across management regimes and incubation durations. Linear regression was used to evaluate trends in soil microbial ecological strategies (oligotrophic *vs*. copiotrophic) in response to cumulative carbon emissions. To explore whether these relationships vary under different management practices, standardized major axis (SMA) regression was applied using the smatr package (Yu *et al.* 2024). Stepwise regression was used to separately analyze the relationships between various respiration variables and potential predictors, including MBC, C-Oxidases, C-Hydrolases, NAG, and AKP.

To understand how microbial communities interact with the dynamics of enzyme activities, Mantel tests, conducted *via* the linkET package, were used to examine the correlation between extracellular enzyme activities and community structure during the long-term incubation. Correlation analyses were performed to investigate the relationships between extracellular enzyme activities and ecological strategies over time. Finally, we used partial least squares path modeling (PLS-PM) to assess the direct and indirect effects of microbial community structure, ecological strategies, and extracellular enzyme activities on the mineralization dynamics of the SOC pools (i.e., changes in SOC quantity and quality). The models were constructed using the "plspm" package (Tian *et al.* 2021). This model accounted for all plausible pathways, and the goodness-of-fit index (GoF) was used to evaluate the overall model fit, with a GoF value of 0.70 or higher indicating a good fit. Unless otherwise specified, all statistical analyses were conducted using R (https://www.r-project.org).

3. Results

3.1. Mineralization dynamics of soil carbon pools during long-term incubation in grassland soils under different management regimes

Soil microbial respiration rates and cumulative carbon emissions showed similar trends in both enclosed and grazed grassland soils throughout the incubation period. Soil respiration rates progressively declined, while cumulative carbon emissions steadily increased (Fig. 3-A and D). The three-pool model applied to the cumulative carbon emissions data demonstrated an excellent fit (R^2=0.999; Fig. 3-D), accurately capturing the mineralization dynamics of the three carbon pools. The contribution of the active (fR1), slow (fR2), and passive (fR3) carbon pool to total respiration changed over time, but displayed similar trends across both management regimes (Fig. 3-B and C). The fR1 decreased rapidly at first, then stabilized, while the fR3 continuously increased. The fR2 gained increasing important as fR1 declined, ultimately becoming the dominant contributor to soil respiration until later in the incubation, when fR3 increased and became the dominant contributor. The proportions of different carbon pools relative to the total carbon pool also shifted during incubation (Fig. 3-E and F), with the active pool (fP1) declining rapidly and the fP3 gradually increasing. Enclosed grasslands showed higher respiration rates and greater cumulative carbon emissions than grazed grasslands (Fig. 3; Appendix B). Notably, respiration rates in enclosed grasslands were significantly higher during the first 113 days (Fig. 3-A; P<0.05) but later converged with those in grazed grasslands. Additionally, enclosed grassland soils had higher proportions of both active carbon pools relative to total carbon compared to grazed soils. The active carbon pool in enclosed soils accounted for 5.74% of the total carbon, approximately 110% greater than the 2.73% in grazed soils (Appendix C).

3.2. Dynamics of extracellular enzyme activities during long-term incubation in grassland soils under different management regimes

Extracellular enzyme activities in both enclosed and grazed grassland soils followed similar trends during the incubation period (Fig. 4; Appendix D). C-Hydrolase activity exhibited a gradual decline, in enclosed soils, decreasing from 443.7 nmol h^{-1} g^{-1} on day 30 to 345.6 nmol h^{-1} g^{-1} on day 553, representing a 22.1% reduction. In grazed soils, activity declined from 365.5 to 339.5 nmol h^{-1} g^{-1}, a 7.1% reduction (Fig. 4-A). In contrast, C-Oxidase activity increased initially, then decreased but remained significantly higher at later stages compared to day 30 (Fig. 4-B; P<0.05). For example, in enclosed soils, C-Oxidase levels increased from a baseline of 1.83 mg h^{-1} g^{-1} on day 30 to 3.60, 2.45, and 2.30 mg h^{-1} g^{-1} on days 185, 366, and 553, corresponding to increases of 96.9, 34.1, and 25.9%, respectively.

Mass-specific hydrolase (MC-Hydrolase) and MC-Oxidase activities steadily increased throughout the incubation in both soil types. By day 553, MC-Oxidase activity increased by 190.6% (from 0.0023 to 0.0066 mg h^{-1} μg^{-1} MBC) in enclosed soils and 256.1% (from 0.0023 to 0.0083 mg h^{-1} μg^{-1} MBC) in grazed soils, while MC-Hydrolase activity increased by 80.6% (from 0.55 to 1.00 nmol h^{-1} μg^{-1} MBC) and 138.3% (from 0.54 to 1.29 nmol h^{-1} μg^{-1} MBC) in enclosed and grazed soils, respectively (Fig. 4-C and D). The ratio of C-Oxidase to C-Hydrolase initially increased and then decreased, but remained significantly higher in later stages than on day 30 (Fig. 4-E; P<0.05). For example, in grazed soils, the ratio increased by 131.8, 135.9, and 51.4% (to 0.0101, 0.0103, 0.0066 mg $nmol^{-1}$) on days 185, 366, and 553, respectively, compared to day 30 (0.0044 mg $nmol^{-1}$). Additionally, the ratios of C-Hydrolase activity to both N- and P-related enzyme

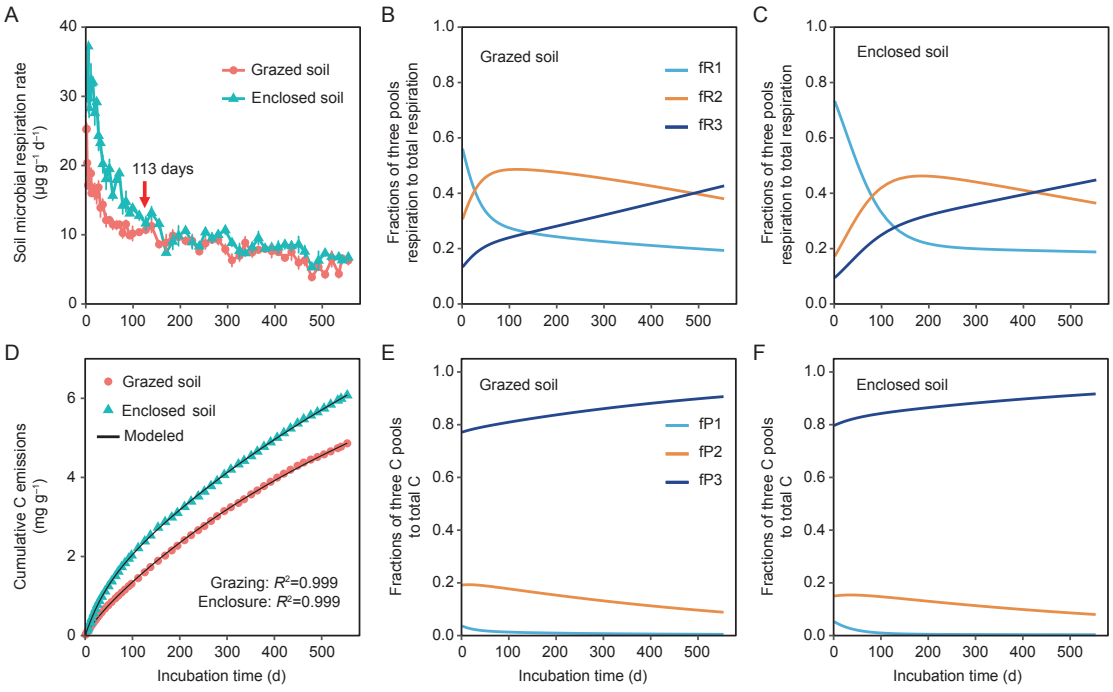

Fig. 3 Dynamics of the three carbon pools during long-term incubation in enclosed and grazed grassland soils. A and D, soil microbial respiration rates (A) and cumulative carbon emissions (D) during long-term incubation in enclosed and grazed grassland soils. Error bars indicate standard errors (n=3). The black line represents modeled data from the three-pool carbon model, with R^2 indicating the model's goodness of fit. B and C, fractions of three pools respiration to total respiration during long-term incubation in grazed (B) and enclosed (C) grassland soils. E and F, fractions of the three C pools to total C during long-term incubation in grazed (E) and enclosed (F) grassland soils. fR1, fR2 and fR3 represent the contributions of active, slow, and passive carbon pools respiration to total respiration, respectively. fP1, fP2 and fP3 represent the fraction of active, slow, and passive carbon pools relative to total carbon, respectively.

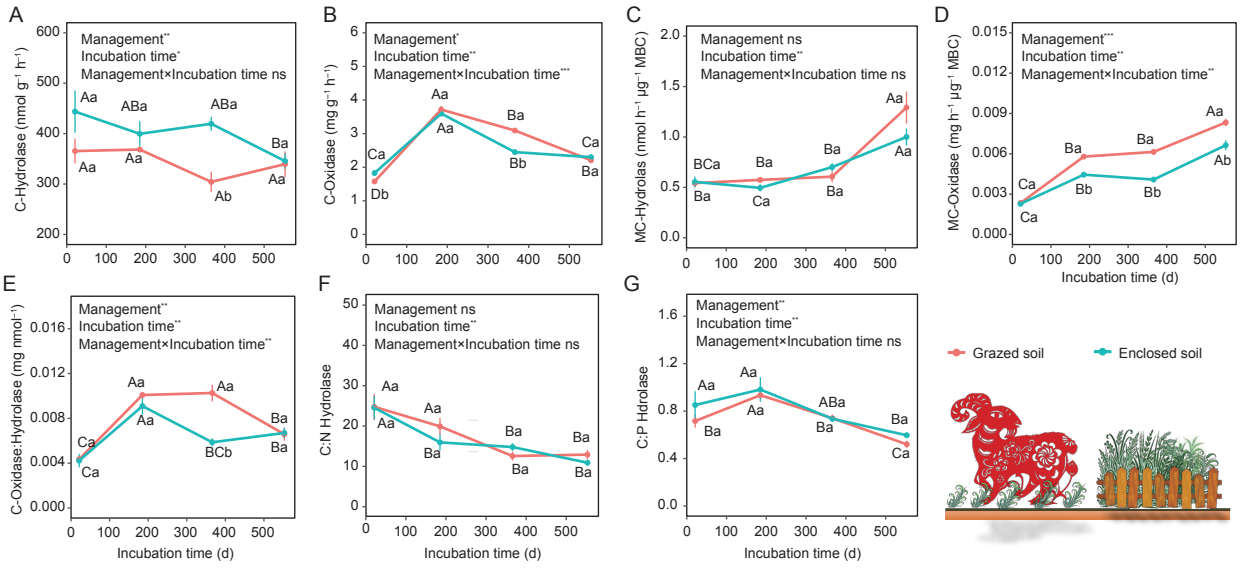

Fig. 4 Changes in potential enzyme activities, mass-specific enzyme activities, and enzyme stoichiometry during long-term incubation of enclosed and grazed grassland soils. MC, mass-specific; MBC, microbial biomass carbon. Management regimes, incubation time, and their interaction were analyzed using a two-way repeated-measures ANOVA. *, P<0.05; **, P<0.01; ***, P<0.001; ns indicates nonsignificant. For detailed statistical values, see Appendix E. Error bars indicate standard errors (n=3). Different uppercase letters indicate significant differences between incubation days, while different lowercase letters indicate significant differences between grazed and enclosed treatments (Fisher's LSD, α=0.05).

(NAG and AKP) activities decreased over time (Fig. 4-F and G).

Overall, enclosed soils showed higher hydrolytic enzyme activities and microbial biomass, while grazed soils had higher oxidative enzyme activities and mass-specific enzyme activity

throughout the incubation (Fig. 4; Appendix D). Despite these differences, most enzyme activities and stoichiometric ratios exhibited similar temporal patterns across management regimes, and the interaction effects between management and incubation time were not significant (Appendix E; $P>0.05$).

3.3. Shifts in microbial community composition during long-term incubation in grassland soils under different management regimes

Soil sample analysis identified a total of 5,299 unique bacterial amplicon sequence variants (ASVs) and 1,304 fungal ASVs, which were classified into 23 bacterial and 9 fungal phyla. The Shannon diversity index (based on ASV counts) for bacterial communities significantly decreased in both enclosed and grazed grasslands over the incubation period (Appendix F; $P<0.05$). In contrast, the Shannon index for fungal community remained relatively stable, showing no significant changes over time (Appendix F). PCoA based on Bray-Curtis distances demonstrated distinct shifts in bacterial and fungal community structures under different management regimes over the incubation period (Fig. 5-A and B). Bacterial and fungal communities were distinctly separated in the PCoA plots according to the management regimes. The positions of bacterial and fungal community structures at different incubation times shifted progressively along the PCoA axes, indicating temporal succession. These observations were further supported by Adonis tests (Fig. 5-A and B). For bacterial communities, both management regime (R^2=0.09, P=0.001) and incubation time (R^2=0.57, P=0.001) accounted for significant portions of the variation in community structure. Similarly, for fungal communities, both management (R^2=0.26, P=0.001) and incubation time (R^2=0.39, P=0.001) had significant effects. However, no significant interaction effect between management regimes and incubation time was observed for bacterial communities. Notably, PCoA analysis showed similar trends in the dynamics of microbial community composition dynamics for both enclosed and grazed grasslands throughout the long-term incubation period (Fig. 5-A and B).

At the phylum level, the dominant bacterial taxa (relative abundance>5%) were Proteobacteria, Acidobacteria, Actinobacteria, Bacteroidetes, and Planctomycetes, while the dominant fungi groups were Ascomycota, Basidiomycota, and Mortierellomycota (Fig. 5-C and D). To evaluate the balance between oligotrophic and copiotrophic microorganisms, the ratio of relative abundances of oligotrophic Basidiomycota to copiotrophic Ascomycota was calculated for fungi. For bacteria, the same approach was applied, comparing oligotrophic taxa like Acidobacteria, Actinobacteria, and Planctomycetes with copiotrophic groups such as

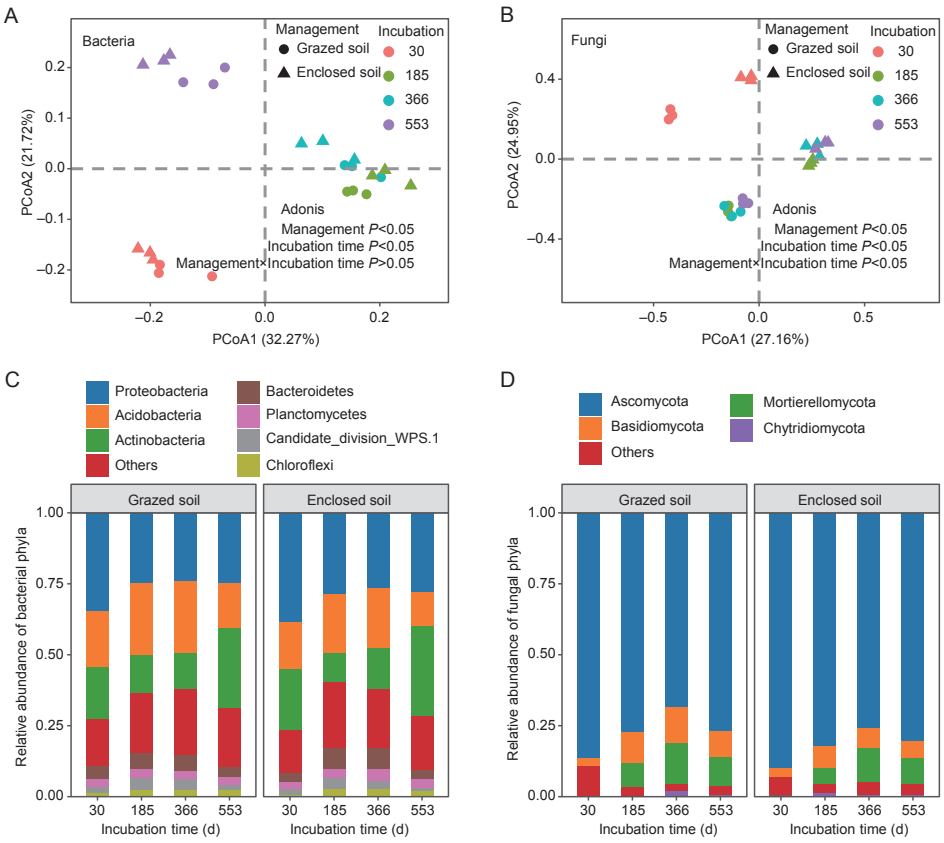

Fig. 5 Changes in microbial community composition in enclosed and grazed grassland soils during long-term incubation. PCoA based on Bray-Curtis distances was used to analyze the soil bacterial (A) and fungal (B) community compositions at the ASV level. The significant effects of management regimes, incubation times, and their interaction on microbial beta diversity were detected by Adonis test. Changes in the relative abundance of different bacterial (C) and fungal (D) phyla under different management regimes and incubation times were also analyzed.

Proteobacteria and Bacteroidetes. Throughout incubation, the relative abundance of oligotrophic bacteria and fungi increased with SOC mineralization (Fig. 6-A and D), while copiotrophic bacteria and fungi decreased (Fig. 6-B and E). By the end of the incubation (day 553), the oligotroph-to-copiotroph ratios in enclosed grasslands had increased by 55.5% for bacteria and 96.9% for fungi compared to the early stage (day 30) (Fig. 6-C and F; Appendix G). In grazed grasslands, these ratios increased by 62.6% for bacteria and 247.5% for fungi (Fig. 6-C and F; Appendix G). The oligotroph-to-copiotroph ratios were lower in enclosed grasslands compared to grazed grasslands (Fig. 6-C and F), with reductions of 16.0% for bacteria and 36.0% for fungi. Standardized major axis (SMA) results indicated no significant differences in the oligotroph-to-copiotroph ratios of bacteria and fungi related to cumulative carbon emissions between management regimes (Fig. 6; P_{dif}>0.05).

3.4. Microbial and enzymatic mechanisms driving mineralization of three soil carbon pools

MBC and key extracellular enzymes involved in SOC mineralization were incorporated into a stepwise regression model to identify the main factors influencing total soil respiration, the respiration rates of the three carbon pools, and their contributions to total respiration. The results indicated that C-Oxidase activity and MBC were the most significant predictors of these variables (Table 1). MBC was significantly positively correlated with total soil respiration, particularly influencing the respiration of the active carbon pool (R1) and its contribution to total respiration (fR1, P<0.05). In contrast, C-Oxidase activity was negatively correlated with total soil respiration, the respiration rates of the active and slow carbon pools (R1 and R2), and the contribution of the active pool to total respiration (fR1). Furthermore, C-Oxidase activity, along with NAG, was positively correlated with the contributions of the slow and passive carbon pools to total respiration (fR2 and fR3).

PLS-PM of microbial community composition, microbial ecological strategies (bacterial and fungal oligotroph-to-copiotroph ratios), and extracellular enzyme activities (C-Hydrolase, C-Oxidase, NAG, AKP) explained 86% of the variance in carbon pools during long-term incubation, indicating a robust model fit (GoF=0.70; Fig. 7). Enclosure treatments significantly increased the proportion of copiotrophic microorganisms, while long-term incubation significantly raised the proportion of oligotrophic microorganisms (P<0.05). Among the variables, extracellular enzyme activities had the largest direct effect on carbon pool variance, with a path coefficient of 0.52. Microbial ecological strategies also had a direct positive effect on carbon pool variance (path coefficient=0.30). Shifts in microbial ecological strategies indirectly influenced carbon pool mineralization by modulating extracellular enzyme activities. Mantel and correlation analyses further indicated close associations between microbial community composition, ecological strategies, and extracellular enzyme activities, as well as their stoichiometric ratios (Appendices H and I). The bacterial and fungal oligotroph-to-copiotroph ratios were

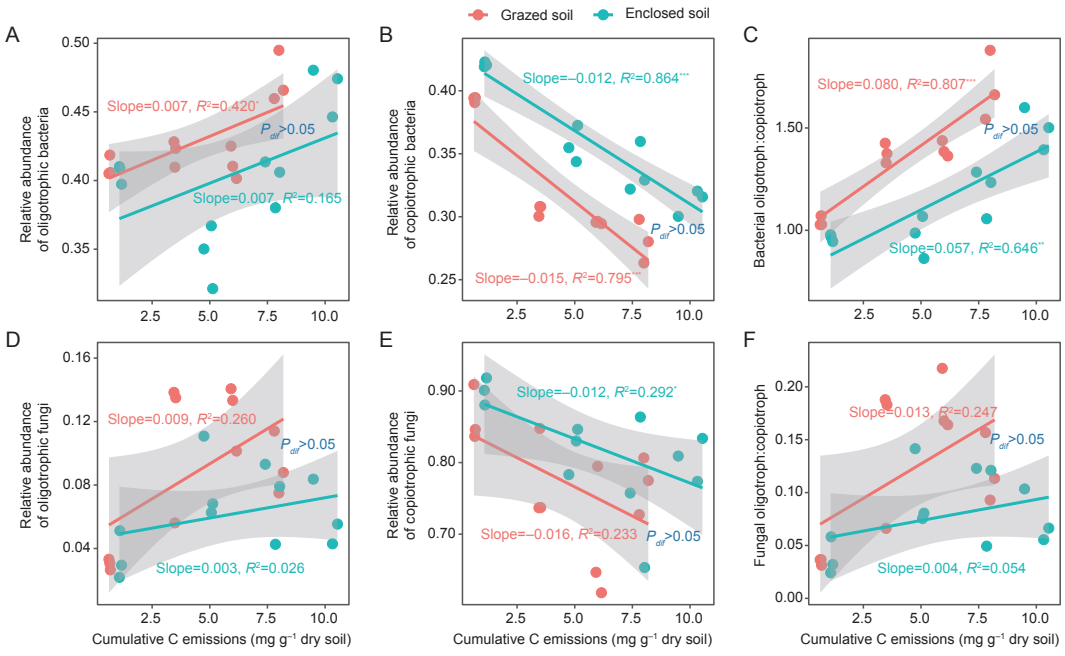

Fig. 6 Shifts in microbial ecological strategies during long-term carbon mineralization in enclosed and grazed grassland soils. A–C, changes in the relative abundance of bacterial oligotrophs (A), copiotrophs (B), and their ratio (C) during long-term carbon mineralization. D–F, changes in the relative abundance of fungal oligotrophs (D), copiotrophs (E), and their ratio (F). Statistical analysis was performed using a linear regression model with two-sided tests, and adjusted R^2 values were reported. Significance levels for the linear regression model are indicated by asterisks (*, P<0.05, **, P<0.01, ***, P<0.001). Gray shading indicates the 95% confidence intervals. Differences in the slopes of the linear relationships between management regimes were compared using the standardized major axis analysis (SMA), with significant differences indicated by P_{dif}<0.05.

Table 1 Stepwise regression models predicting various respiration variables, including total respiration, respiration rates of the three carbon pools (R), and their relative contribution to total respiration (fR)

	Regression equation[1)]	R^2	*P*-value
Soil respiration	SR=–5.314C-Oxidase+0.025MBC+16.953	0.706	<0.0001
R	R1=–4.066×10^{-3}C-Oxidase+1.801×10^{-5}MBC+4.267×10^{-3}	0.667	<0.0001
	R2=–4.986×10^{-4}C-Oxidase–7.360×10^{-5}NAG+5.862×10^{-6}MBC+3.721×10^{-3}	0.942	<0.0001
	R3=3.500×10^{-5}NAG+1.860×10^{-6}AKP+2.169×10^{-6}MBC–1.677×10^{-4}	0.722	<0.0001
fR	fR1=–0.1162C-Oxidase-6.944×10^{-3}NAG+4.363×10^{-4}MBC+0.504	0.777	<0.0001
	fR2=6.765×10^{-2}C-Oxidase+0.328	0.554	<0.0001
	fR3=5.535×10^{-2}C-Oxidase+7.633×10^{-3}NAG -3.053×10^{-4}MBC+7.117×10^{-2}	0.901	<0.0001

[1)] SR, total respiration rate; R1, respiration rate of the active carbon pool; R2, respiration rate of the slow carbon pool; R3, respiration rate of the passive carbon pool; fR1, contribution of the active carbon pool to total respiration; fR2, contribution of the slow carbon pool to total respiration; fR3, contribution of the passive carbon pool to total respiration; MBC, microbial biomass carbon; C-oxidase, carbon oxidase; C-hydrolase, carbon hydrolase; NAG, N-acetylglucosaminidase; AKP, alkaline phosphatase. Potential predictors include MBC, C-oxidase, C-hydrolase, NAG and AKP. The analysis spanned a 553-day incubation period, with carbon pools categorized as active, slow, and passive.

significantly negatively correlated with soil respiration (P<0.05) and positively correlated with soil C-Oxidase:Hydrolase, MC-Hydrolase, MC-Oxidase, and NAG activities (P<0.05). Furthermore, MC-Hydrolase and MC-Oxidase activities were significantly negatively correlated with NAG activity (Appendix H; P<0.05).

4. Discussion

4.1. Changes in soil carbon pools and mineralization rates during long-term incubation of grassland soils

This 553-day incubation study provided valuable insights into the long-term dynamics of soil carbon pools, highlighting the critical transition from the rapid mineralization of active carbon to the slower breakdown of stable carbon fractions — processes that are often overlooked in shorter-term studies. By monitoring high-resolution soil respiration and applying the three-pool model, this study offers a comprehensive understanding of how soil carbon processes evolve under different grassland management regimes over extended periods.

Our results showed a significant decline in microbial respiration rates in both enclosed and grazed grassland soils as the incubation progressed, particularly during the first 113 days (Fig. 3). This reduction was primarily driven by the rapid depletion of active carbon, as confirmed by the three-pool model (Fig. 3). This finding aligns with our first hypothesis, which predicted that the active carbon pool would be quickly exhausted, leading to the development of a more complex SOC structure. The decreased substrate availability also resulted in a reduction in microbial biomass (Appendix D), which further contributed to the overall decline in total soil respiration, particularly from the active carbon pool (Table 1). This shift is consistent with previous incubation studies (Feng *et al.* 2017; Zhang and Zhou 2018), which emphasize the growing importance of stable SOC fractions, such as mineral-associated and aggregate-protected carbon, in regulating total respiration during the later stages of long-term mineralization (Plante and McGill 2002; Giannetta *et al.* 2018).

During the early stages of incubation, enclosed soils exhibited higher respiration rates and carbon emissions compared to grazed grasslands (Fig. 3; Appendix B), indicating differences in carbon pool composition between the

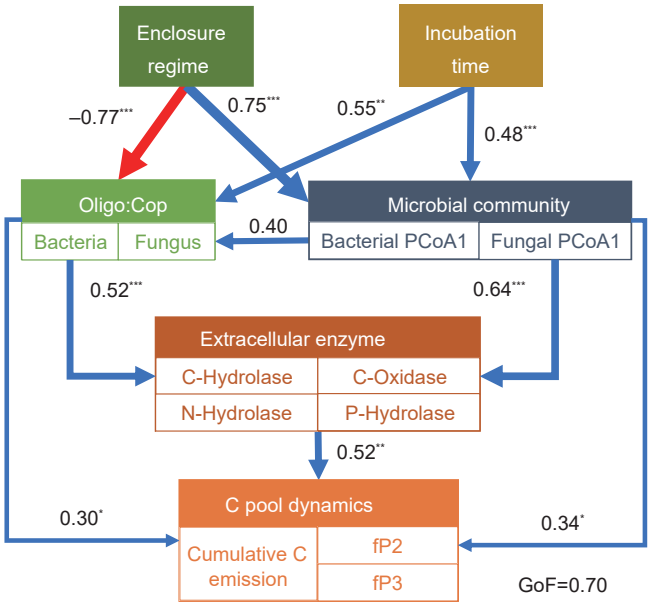

Fig. 7 Mechanisms regulating soil carbon pool dynamics in grazed and enclosed grasslands during long-term incubation. Partial least squares path modeling (PLS-PM) indicating the relationships between soil microbial community structure, extracellular enzyme activities, and carbon pools. GoF, goodness of fit of the model. Blue and red arrows indicate positive and negative relationships, with the thickness of the line and the numbers indicating the magnitude of the standardized coefficients. *, P<0.05, **, P<0.01, ***, P<0.001. Oligo:Cop, oligotroph to copiotroph ratio of bacteria and fungi. fP2 and fP3 represent the fraction of slow and passive carbon pools relative to total carbon pool, respectively.

two management regimes. This disparity can be attributed to reduced disturbance, increased plant residue inputs, and enhanced microbial activity in enclosed grasslands (Xiong *et al.* 2016; Bai *et al.* 2021). Enclosed soils also showed higher microbial biomass, elevated hydrolytic enzyme activities, and a greater abundance of copiotrophic microorganisms (Figs. 4 and 6), which collectively contributed to increased carbon substrate availability in these systems. However, as the incubation progressed, differences in respiration rates between the two regimes diminished (Fig. 3), supporting our third hypothesis that mineralization dynamics would converge over time. This convergence is likely driven

by the gradual depletion of labile carbon pools, which reduces the differences in substrate complexity between enclosed and grazed soils.

4.2. Microbial communities drive soil carbon three pool mineralization dynamics by regulating extracellular enzymes

While similar trends in the variation of the three carbon pools and converging microbial respiration patterns were observed between enclosed and grazed soils during incubation (Fig. 3), the parallel shifts in enzyme activity, microbial community composition, and ecological strategies (Figs. 4–6) suggest that both grassland systems share common underlying mechanisms driving SOC mineralization. Our findings demonstrated that over time, the microbial community transitioned from a copiotrophic to an oligotrophic strategy, accompanied by significant changes in enzyme activity — specifically, an increase in C-Oxidase activity and a decrease in C-Hydrolase activity. These microbial and enzymatic shifts are strongly correlated with changes in carbon pool fractions (Fig. 6), indicating that they serve as the primary drivers of SOC mineralization under both management regimes, supporting our second and third hypotheses.

Microorganisms adopt distinct ecological strategies, such as copiotroph and oligotroph, to decompose different carbon substrates and meet their metabolic and energy demands. Copiotrophic microbes (r-strategists) thrive in carbon-rich environments, driving rapid mineralization, while oligotrophic microbes (K-strategists) are more efficient at degrading recalcitrant carbon over extended periods (Fierer *et al.* 2007; Ho *et al.* 2017; Peng *et al.* 2025). These microbial strategies not only affect substrate properties but are also shaped by them (Bernhardt *et al.* 2022), creating a feedback loop that influences soil respiration and broader ecosystem processes. In our study, we assessed the transition in microbial ecological strategies during incubation by examining the ratio of oligotrophs to copiotrophs within bacterial and fungal communities. The increase in oligotroph-to-copiotroph ratios (Fig. 6), combined with the negative correlation between these ratios and soil respiration (Appendix I), indicates that shifts in microbial strategies significantly influence SOC mineralization rates. A higher relative abundance of oligotrophic microorganisms is associated with lower soil respiration (Qiu *et al.* 2023). This pattern may also explain why grazed grassland soils exhibited lower soil respiration and carbon emissions compared to enclosed soils, as grazed soils maintained a higher oligotroph-to-copiotroph ratio (Fig. 6).

In the PLS-PM analysis, extracellular enzyme activities had the strongest direct effect on carbon pool variance, with a path coefficient of 0.52, compared to the effect of microbial ecological strategies, which had a direct path coefficient of 0.30 (Fig. 7). This finding is consistent with previous studies showing that microbial-derived enzymes contribute to nearly half of CO_2 emissions from decomposing SOC, even under soil sterilization conditions, emphasizing the critical role of enzymes in soil respiration (Maire *et al.* 2013). Throughout the incubation, we observed a significant increase in C-Oxidase activity (Fig. 4) and a positive correlation between C-Oxidase and the contribution of slow and passive carbon pools to total respiration (Table 1). Additionally, the positive correlation between the C-Oxidase:Hydrolase and the oligotroph-to-copiotroph ratio (Appendix I) suggests that shifts in microbial ecological strategies are tightly linked to changes in enzyme activity, driving the utilization of different carbon pools. Copiotrophic microorganisms thrive in environments rich in labile carbon, whereas oligotrophic microorganisms excel at utilizing recalcitrant carbon (Fierer *et al.* 2007). During the early incubation phase, copiotrophic taxa, such as Proteobacteria, might upregulated the secretion of hydrolytic enzymes (e.g., BG, BXYL) to rapidly mineralize the active carbon pool, aligning with their preference for readily degradable substrates. As the incubation progressed and the labile carbon pool became depleted, oligotrophic lineages such as, *Actinobacteria*, gradually became dominant. These taxa enhanced the production of oxidative enzymes (e.g., PPO, PER), thereby facilitating the decomposition of complex substrates — such as lignin and aromatic compounds — within the slow and passive carbon pools (Chen *et al.* 2018; Peng *et al.* 2025). Notably, the fungal oligotroph-to-copiotroph ratio showed a stronger positive correlation with both C-Oxidase activity and the C-Oxidase:Hydrolase compared to bacteria, further supporting the notion that fungi are more efficient at decomposing recalcitrant carbon and are the primary producers of oxidases (Navarro *et al.* 2014; Treseder and Lennon 2015; Schalk *et al.* 2021). For example, fungi, particularly white-rot fungi, utilize enzymes such as peroxidases to degrade complex and persistent lignin compounds (Gałązka *et al.* 2025).

Moreover, variations in mass-specific enzyme (MC-Oxidase and MC-Hydrolase) activities, as well as N- and P-acquisition enzymes (NAG and AKP), also help explain carbon pool variance. We observed progressively increasing MC-Oxidase and MC-Hydrolase activities throughout the incubation (Fig. 4-C and D), along with a significant positive correlation between these activities and the oligotroph-to-copiotroph ratio (Appendix I). These findings are consistent with microbial economic theories, which suggest that microorganisms may allocate more resources to enzyme production in response to the low availability and quality of soil substrates (Zhang *et al.* 2023). Notably, MC-Oxidase activity displayed the highest sensitivity during incubation (Fig. 4-D), underscoring the critical role of C-Oxidative enzymes in driving the mineralization of soil carbon pools during extended incubation periods. Interestingly, N- and P-related enzymes activities and demand also increased over time (Fig. 4; Appendix D), and a positive correlation was observed between these enzyme activities and the mineralization of passive carbon pools (Table 1). This suggests that N- and P-related enzymes also play a role in passive carbon mineralization. The underlying reason may be twofold: first, to meet the increasing demand for enzyme synthesis, as enzymes are protein-based and require nitrogen; second, to adapt to the accumulation of nitrogen and phosphorus in soil organic matter over time (Hilscher *et al.* 2009; Chen *et al.* 2024). Some studies support this, showing that while NAG and LAP are primarily involved in

nitrogen acquisition, they can also contribute to C acquisition when protein, chitin, and peptidoglycan become dominant carbon sources (Mori 2020). In summary, our study suggests that both enclosed and grazed grassland soils share similar mechanisms driving carbon mineralization. Microbial communities adapt their ecological strategies by reallocating resources and investing in enzyme production, enabling them to efficiently extract energy and nutrients from increasingly recalcitrant carbon substrates during long-term incubation.

4.3. Limitations and future directions

The integration of a three-pool model with analyses of soil microbial community and enzyme activities during long-term incubation offers valuable insights into the dynamics of soil carbon pool mineralization and the underlying mechanisms. While our findings advance the understanding of these processes, several important limitations must be acknowledged. Firstly, the three-pool model, which widely used in soil respiration research, has inherent simplifications. It assumes discrete carbon pools and first-order decay kinetics, which may not fully capture the continuum nature of SOC decomposition. In addition, the model does not explicitly account for microbial physiology, enzyme kinetics, or interactions with soil structure, meaning that certain microbially driven processes may be underrepresented (Guan *et al.* 2022; Guo *et al.* 2022). Secondly, the controlled laboratory conditions do not accurately replicate the environmental variability observed in natural ecosystems. In field settings, temperature and moisture fluctuate seasonally and with weather changes, leading to significant variations in microbial activity and SOC mineralization rates. While our incubation approach was ideal for isolating microbial mechanisms without confounding environmental factors (Huo *et al.* 2017; Ma *et al.* 2019), caution should be exercised when extrapolating the absolute mineralization rates reported here to field conditions. Moreover, the ecological complexity of natural systems — including interactions among plant roots, soil fauna, and microbial communities — plays a critical role in SOC mineralization (Bardgett and van der Putten 2014; Kuzyakov and Blagodatskaya 2015; Wang B *et al.* 2020). This complexity can obscure or even reverse the observed relationships between microbial community composition and extracellular enzyme activity in natural field conditions (Li *et al.* 2024).

To address these limitations, several approaches can be considered. Firstly, the application of functional genomics and metabolomics would help investigate the dynamics of key genes and metabolic pathways involved in carbon catabolism, offering deeper mechanistic insights into microbial responses to different carbon pools (Delgado-Baquerizo *et al.* 2018). Secondly, a more in-depth exploration of microbial physiological traits — such as carbon use efficiency, growth rates, and adaptability in utilizing various carbon substrates (Tao *et al.* 2023) — would provide a better understanding of microbial allocation and competitiveness in diverse environments. Thirdly, future research should incorporate long-term field experiments to validate and extend the applicability of laboratory findings (Smith *et al.* 2016). Finally, collecting high-resolution temporal and spatial data on microbial activity, enzyme kinetics, and SOC fractions will significantly improve model calibration and validation. This will not only enhance our understanding of SOC mineralization mechanisms but also improve carbon cycle predictions (Jian *et al.* 2020).

5. Conclusion

In this study, we investigated the mineralization dynamics of the three pools of SOC in grasslands under different management regimes, with a focus on the roles of microbial communities and extracellular enzyme activities. Our findings underscored the critical role of extracellular enzyme patterns, which are driven by shifts in microbial ecological strategies in the mineralization of SOC pools — particularly the transition from copiotrophic to oligotrophic microbial communities during long-term incubation. While enclosure accelerated initial SOC mineralization rates (significantly higher during the first 113 days), the management regimes did not significantly alter the long-term mineralization mechanisms of the soil carbon pool. The study further highlighted that, in addition to oxidative enzymes, mass-specific enzyme activities and N and P-Hydrolase are essential for sustaining microbial metabolism and facilitating the mineralization of recalcitrant carbon pools as nutrient demands increase during labile carbon depletion. These insights deepen our understanding of the microbially-driven mechanisms underlying SOC decomposition and provide valuable guidance for optimizing grassland management practices — for example, by prioritizing policies that protect and stabilize carbon in slow and passive pools through practices such as minimizing soil disturbance and promoting plant diversity — thereby enhancing carbon sequestration and mitigating climate change.

Acknowledgements

This study was funded by the National Natural Science Foundation of China (42377471), the Natural Science Foundation of Ningxia Hui Autonomous Region, China (2024A AC05099), and the Open Project of Key Laboratory of the Alpine Grassland Ecology in the Three Rivers Region (2023-SJY-KF-04) from Qinghai University, China.

Declaration of competing interest

The authors declare that they have no conflict of interest.

Declaration of generative AI and AI-assisted technologies in scientific writing

The authors declare that they did not use AI in the preparation and writing of this manuscript.

Appendices associated with this paper are available at https://doi.org/10.1016/j.jia.2025.12.030

References

Andren O, Paustian K. 1987. Barley straw decomposition in the field: A comparison of models. *Ecology*, **68**, 1190–1200.

Bai X, Yang X, Zhang S, An S. 2021. Newly assimilated carbon allocation

in grassland communities under different grazing enclosure times. *Biology and Fertility of Soils*, **57**, 563–574.
Bai Y, Cotrufo M F. 2022. Grassland soil carbon sequestration: Current understanding, challenges, and solutions. *Science*, **377**, 603–608.
Bardgett R D, van der Putten W H. 2014. Belowground biodiversity and ecosystem functioning. *Nature*, **515**, 505–511.
Bernhardt L T, Smith R G, Grandy A S, Mackay J E, Warren N D, Geyer K M, Ernakovich J G. 2022. Soil microbial communities vary in composition and functional strategy across soil aggregate size class regardless of tillage. *Elementa*: *Science of the Anthropocene*, **10**, 00023.
Birge H E, Conant R T, Follett R F, Haddix M L, Morris S J, Snapp S S, Wallenstein M D, Paul E A. 2015. Soil respiration is not limited by reductions in microbial biomass during long-term soil incubations. *Soil Biology and Biochemistry*, **81**, 304–310.
Chen G, Yuan J, Chen H, Wang L, Wang S, Wang Y. 2024. Manure application influences microbial stoichiometry and alters microbial life strategies to regulate phosphorus bioavailability in low-P paddy soil. *Soil and Tillage Research*, **244**, 106241.
Chen J, Elsgaard L, van Groenigen K J, Olesen J E, Liang Z, Jiang Y, Lærke P E, Zhang Y, Luo Y, Hungate B A, Sinsabaugh R L, Jørgensen U. 2020. Soil carbon loss with warming: New evidence from carbon-degrading enzymes. *Global Change Biology*, **26**, 1944–1952.
Chen J, Luo Y, García-Palacios P, Cao J, Dacal M, Zhou X, Li J, Xia J, Niu S, Yang H, Shelton S, Guo W, van Groenigen K J. 2018. Differential responses of carbon-degrading enzyme activities to warming: implications for soil respiration. *Global Change Biology*, **24**, 4816–4826.
Delgado-Baquerizo M, Maestre F T, Reich P B, Jeffries T C, Gaitan J J, Encinar D, Berdugo M, Campbell C D, Singh B K. 2016. Microbial diversity drives multifunctionality in terrestrial ecosystems. *Nature Communications*, **7**, 10541.
Delgado-Baquerizo M, Oliverio A M, Brewer T E, Benavent-González A, Eldridge D J, Bardgett R D, Maestre F T, Singh B K, Fierer N. 2018. A global atlas of the dominant bacteria found in soil. *Science*, **359**, 320–325.
Domínguez M T, Holthof E, Smith A R, Koller E, Emmett B A. 2017. Contrasting response of summer soil respiration and enzyme activities to long-term warming and drought in a wet shrubland (NE Wales, UK). *Applied Soil Ecology*, **110**, 151–155.
Feng W, Liang J, Hale L E, Jung C G, Chen J, Zhou J, Xu M, Yuan M, Wu L, Bracho R, Pegoraro E, Schuur E A G, Luo Y. 2017. Enhanced decomposition of stable soil organic carbon and microbial catabolic potentials by long-term field warming. *Global Change Biology*, **23**, 4765–4776.
Feyisa K, Beyene S, Angassa A, Said M Y, de Leeuw J, Abebe A, Megersa B. 2017. Effects of enclosure management on carbon sequestration, soil properties and vegetation attributes in East African rangelands. *Catena*, **159**, 9–19.
Fierer N. 2017. Embracing the unknown: Disentangling the complexities of the soil microbiome. *Nature Reviews Microbiology*, **15**, 579–590.
Fierer N, Bradford M A, Jackson R B. 2007. Toward an ecological classification of soil bacteria. *Ecology*, **88**, 1354–1364.
Gałązka A, Jankiewicz U, Orzechowski S. 2025. The role of ligninolytic enzymes in sustainable agriculture: Applications and challenges. *Agronomy*, **15**, 451.
Gelman A, Rubin D B. 1992. Inference from iterative simulation using multiple sequences. *Statistical Science*, **7**, 457–472.
German D, Weintraub M, Grandy S, Lauber C, Rinkes Z, Allison S. 2011. Optimization of hydrolytic and oxidative enzyme methods for ecosystem studies. *Soil Biology and Biochemistry*, **43**, 1387–1397.
Giannetta B, Plaza C, Vischetti C, Cotrufo M F, Zaccone C. 2018. Distribution and thermal stability of physically and chemically protected organic matter fractions in soils across different ecosystems. *Biology and Fertility of Soils*, **54**, 671–681.
Guan X, Jiang J, Jing X, Feng W, Luo Z, Wang Y, Xu X, Luo Y. 2022. Optimizing duration of incubation experiments for understanding soil carbon decomposition. *Geoderma*, **428**, 116225.
Guo D, Li X, Wang J, Niu D, Guo W, Fu H, Luo Y. 2020. Edaphic and microbial determinants of the residence times of active and slow C pools on the Tibetan Plateau. *Geoderma*, **357**, 113942.
Guo D, Wang J, Fu H, Wen H, Luo Y. 2017. Cropland has higher soil carbon residence time than grassland in the subsurface layer on the Loess Plateau, China. *Soil and Tillage Research*, **174**, 130–138.
Guo X, Viscarra Rossel R A, Wang G, Xiao L, Wang M, Zhang S, Luo Z. 2022. Particulate and mineral-associated organic carbon turnover revealed by modelling their long-term dynamics. *Soil Biology and Biochemistry*, **173**, 108780.
Guo X, Yan M, Huang D, Chen S, Zhang D, Li Z, Yang X, Wu W. 2023. A large scale 16S ribosomal RNA gene amplicon dataset of hand, foot and mouth patients and healthy individuals. *Scientific Data*, **10**, 48.
Hastings W K. 1970. Monte Carlo sampling methods using Markov chains and their applications. *Biometrika*, **57**, 97–109.
Hilscher A, Heister K, Siewert C, Knicker H. 2009. Mineralisation and structural changes during the initial phase of microbial degradation of pyrogenic plant residues in soil. *Organic Geochemistry*, **40**, 332–342.
Ho A, Di Lonardo D P, Bodelier P L E. 2017. Revisiting life strategy concepts in environmental microbial ecology. *FEMS Microbiology Ecology*, **93**, fix006.
Hu J, Cui Y, Manzoni S, Zhou S, Cornelissen J H C, Huang C, Schimel J, Kuzyakov Y. 2025. Microbial carbon use efficiency and growth rates in soil: Global patterns and drivers. *Global Change Biology*, **31**, e70036.
Huo C, Luo Y, Cheng W. 2017. Rhizosphere priming effect: A meta-analysis. *Soil Biology and Biochemistry*, **111**, 78–84.
Jian S, Li J, Wang G, Kluber L A, Schadt C W, Liang J, Mayes M A. 2020. Multi-year incubation experiments boost confidence in model projections of long-term soil carbon dynamics. *Nature Communications*, **11**, 5864.
Kittredge H A, Cannone T, Funk J, Chapman S K. 2018. Soil respiration and extracellular enzyme production respond differently across seasons to elevated temperatures. *Plant and Soil*, **425**, 351–361.
Koranda M, Rinnan R, Michelsen A. 2023. Close coupling of plant functional types with soil microbial community composition drives soil carbon and nutrient cycling in tundra heath. *Plant and Soil*, **488**, 551–572.
Kuzyakov Y, Blagodatskaya E. 2015. Microbial hotspots and hot moments in soil: Concept & review. *Soil Biology and Biochemistry*, **83**, 184–199.
Li H, Yang S, Semenov M V, Yao F, Ye J, Bu R, Ma R, Lin J, Kurganova I, Wang X, Deng Y, Kravchenko I, Jiang Y, Kuzyakov Y. 2021. Temperature sensitivity of SOM decomposition is linked with a K-selected microbial community. *Global Change Biology*, **27**, 2763–2779.
Li J, Jian S, de Koff J P, Lane C S, Wang G, Mayes M A, Hui D. 2018. Differential effects of warming and nitrogen fertilization on soil respiration and microbial dynamics in switchgrass croplands. *Global Change Biology Bioenergy*, **10**, 565–576.
Li J, Pei J, Fang C, Li B, Nie M. 2023. Thermal adaptation of microbial respiration persists throughout long-term soil carbon decomposition. *Ecology Letters*, **26**, 1803–1814.
Li Y, Ma J, Li Y, Shen X, Xia X. 2024. Microbial community and enzyme activity respond differently to seasonal and edaphic factors in forest and grassland ecosystems. *Applied Soil Ecology*, **194**, 105167.
Liang J, Li D, Shi Z, Tiedje J M, Zhou J, Schuur E A G, Konstantinidis K T, Luo Y. 2015. Methods for estimating temperature sensitivity of soil organic matter based on incubation data: A comparative evaluation. *Soil Biology and Biochemistry*, **80**, 127–135.
Liu L, Sayer E J, Deng M, Li P, Liu W, Wang X, Yang S, Huang J, Luo J, Su Y, Grünzweig J M, Jiang L, Hu S, Piao S. 2023. The grassland carbon cycle: Mechanisms, responses to global changes, and potential contribution to carbon neutrality. *Fundamental Research*, **3**, 209–218.
Liu X, Wang Y, Fu W, Yuan Z, Yu Q, Peng C, Koerner S E, Guo L. 2023. Growing season temperature and precipitation affect nutrient resorption in herbaceous species through a foliar stoichiometric control strategy. *Plant and Soil*, **493**, 45–60.
Liu Y, Zhao X, Yang X, Liu W, Feng B, Sun S, Dong Q. 2025. Yak and Tibetan sheep mixed grazing enhances plant functional diversity in alpine grassland. *Journal of Integrative Agriculture*, **24**, 936–948.
Luo Y, Zhou X. 2006. *Soil Respiration and the Environment*. Elsevier, Burlington.
Ma Y, McCormick M K, Szlavecz K, Filley T R. 2019. Controls on soil organic carbon stability and temperature sensitivity with increased aboveground litter input in deciduous forests of different forest ages. *Soil Biology and Biochemistry*, **134**, 90–99.
Maire V, Alvarez G, Colombet J, Comby A, Despinasse R, Dubreucq E, Joly M, Lehours A-C, Perrier V, Shahzad T, Fontaine S. 2013. An unknown oxidative metabolism substantially contributes to soil CO_2

emissions. *Biogeosciences*, **10**, 1155–1167.
Melillo J M, Frey S D, DeAngelis K M, Werner W J, Bernard M J, Bowles F P, Pold G, Knorr M A, Grandy A S. 2017. Long-term pattern and magnitude of soil carbon feedback to the climate system in a warming world. *Science*, **358**, 101–105.
Metropolis N, Rosenbluth A W, Rosenbluth M N, Teller A H, Teller E. 1953. Equation of state calculations by fast computing machines. *The Journal of Chemical Physics*, **21**, 1087–1092.
Mori T. 2020. Does ecoenzymatic stoichiometry really determine microbial nutrient limitations? *Soil Biology and Biochemistry*, **146**, 107816.
Navarro D, Rosso M, Haon M, Olivé C, Bonnin E, Lesage-Meessen L, Chevret D, Coutinho P, Henrissat B, Berrin J. 2014. Fast solubilization of recalcitrant cellulosic biomass by the basidiomycete fungus Laetisaria arvalis involves successive secretion of oxidative and hydrolytic enzymes. *Biotechnology for Biofuels*, **7**, 143.
Peng Y, Yan Y, Fan Z, Shi J, Huo C, Zhang Z, Wang X. 2025. Microbial associations with soil organic carbon pool composition and stabilization in eroding landscapes. *Catena*, **258**, 109302.
Plante A F, McGill W B. 2002. Soil aggregate dynamics and the retention of organic matter in laboratory-incubated soil with differing simulated tillage frequencies. *Soil and Tillage Research*, **66**, 79–92.
Qiu Y, Zhang K, Zhao Y, Zhao Y, Wang B, Wang Y, He T, Xu X, Bai T, Zhang Y, Hu S. 2023. Climate warming suppresses abundant soil fungal taxa and reduces soil carbon efflux in a semi-arid grassland. *mLife*, **2**, 389–400.
Qu Q, Deng L, Shangguan Z, Sun J, He J, Wang K, Zhou Z, Li J, Penuelas J. 2024. Belowground C sequestrations response to grazing exclusion in global grasslands: Dynamics and mechanisms. *Agriculture Ecosystems and Environment*, **360**, 108771.
Rousk J, Frey S D, Bååth E. 2012. Temperature adaptation of bacterial communities in experimentally warmed forest soils. *Global Change Biology*, **18**, 3252–3258.
Schädel C, Beem-Miller J, Aziz Rad M, Crow S E, Hicks Pries C E, Ernakovich J, Hoyt A M, Plante A, Stoner S, Treat C C, Sierra C A. 2020. Decomposability of soil organic matter over time: The Soil Incubation Database (SIDb, version 1.0) and guidance for incubation procedures. *Earth System Science Data*, **12**, 1511–1524.
Schalk F, Gostinčar C, Kreuzenbeck N B, Conlon B H, Sommerwerk E, Rabe P, Burkhardt I, Krüger T, Kniemeyer O, Brakhage A, Gunde-Cimerman N, de Beer Z D, Dickschat J S, Poulsen M, Beemelmanns C. 2021. The termite fungal cultivar Termitomyces combines diverse enzymes and oxidative reactions for plant biomass conversion. *mBio*, **12**, e0355120.
Smith P, House J I, Bustamante M, Sobocká J, Harper R, Pan G, West P C, Clark J M, Adhya T, Rumpel C, Paustian K, Kuikman P, Cotrufo M F, Elliott J A, McDowell R, Griffiths R I, Asakawa S, Bondeau A, Jain A K, Meersmans J, *et al.* 2016. Global change pressures on soils from land use and management. *Global Change Biology*, **22**, 1008–1028.
Steinweg J M, Dukes J S, Paul E A, Wallenstein M D. 2013. Microbial responses to multi-factor climate change: Effects on soil enzymes. *Frontiers in Microbiology*, **4**, 00146.
Tang Y, Zhou C, Chen K, Xing S, Shi H, Li C, Wang Y, Cui X, Niu H, Ji B, Zhang J. 2025. Grazing exclusion enriches arbuscular mycorrhizal fungal communities and improves soil organic carbon sequestration in the alpine steppe of northern Xizang. *Journal of Integrative Agriculture*, **24**, 913–924.
Tao F, Huang Y, Hungate B A, Manzoni S, Frey S D, Schmidt M W I, Reichstein M, Carvalhais N, Ciais P, Jiang L, Lehmann J, Wang Y, Houlton B Z, Ahrens B, Mishra U, Hugelius G, Hocking T D, Lu X, Shi Z, Viatkin K, *et al.* 2023. Microbial carbon use efficiency promotes global soil carbon storage. *Nature*, **618**, 981–985.
Tian J, Zong N, Hartley I P, He N, Zhang J, Powlson D, Zhou J, Kuzyakov Y, Zhang F, Yu G, Dungait J A J. 2021. Microbial metabolic response to winter warming stabilizes soil carbon. *Global Change Biology*, **27**, 2011–2028.
Treseder K, Lennon J. 2015. Fungal traits that drive ecosystem dynamics on land. *Microbiology and Molecular Biology Reviews*, **79**, 243–262.
Trumbore S E. 1997. Potential responses of soil organic carbon to global environmental change. *Proceedings of the National Academy of Sciences of the United States of America*, **94**, 8284–8291.
Vance E D, Brookes P C, Jenkinson D S. 1987. An extraction method for measuring soil microbial biomass C. *Soil Biology and Biochemistry*, **19**, 703–707.
Wang B, Wu L, Chen D, Wu Y, Hu S, Li L, Bai Y. 2020. Grazing simplifies soil micro-food webs and decouples their relationships with ecosystem functions in grasslands. *Global Change Biology*, **26**, 960–970.
Wang H, Li Y Z, He Y, Chen H Y H, Liu X, Gao Y, Zhu W, Xu J, Li Y J, Chen Z, Sun X. 2023. Grazing exclusion facilitates more rapid ecosystem carbon sequestration of degraded grasslands in humid than in arid regions. *Agriculture Ecosystems and Environment*, **353**, 108553.
Wang J, Liu Y, Cao W, Li W, Wang X, Zhang D, Shi S, Pan D, Liu W. 2020a. Effects of grazing exclusion on soil respiration components in an alpine meadow on the north-eastern Qinghai-Tibet Plateau. *Catena*, **194**, 104750.
Wang J, Ren C J, Feng X, Zhang L, Doughty R, Zhao F. 2020a. Temperature sensitivity of soil carbon decomposition due to shifts in soil extracellular enzymes after afforestation. *Geoderma*, **374**, 114426.
Wang L, Luan L, Hou F, Siddique K H M. 2020. Nexus of grazing management with plant and soil properties in northern China grasslands. *Scientific Data*, **7**, 39.
White R P, Murray S, Rohweder M. 2000. *Pilot Analysis of Global Ecosystems*: *Grassland Ecosystems*. World Resources Institute, Washington.
Wu Y, Chen D, Delgado-Baquerizo M, Liu S, Wang B, Wu J, Hu S, Bai Y. 2022. Long-term regional evidence of the effects of livestock grazing on soil microbial community structure and functions in surface and deep soil layers. *Soil Biology and Biochemistry*, **168**, 108629.
Xiong D, Shi P, Zhang X, Zou C B. 2016. Effects of grazing exclusion on carbon sequestration and plant diversity in grasslands of China — a meta-analysis. *Ecological Engineering*, **94**, 647–655.
Xiang D, Wang G, Tian J, Li W. 2023. Global patterns and edaphic-climatic controls of soil carbon decomposition kinetics predicted from incubation experiments. *Nature Communications*, **14**, 2171.
Xiang X, Yao T, Man B, Lin D, Li C. 2024. Global hotspots and trends in microbial-mediated grassland carbon cycling: A bibliometric analysis. *Frontiers in Microbiology*, **15**, 1377338.
Xu T, White L, Hui D, Luo Y. 2006. Probabilistic inversion of a terrestrial ecosystem model: Analysis of uncertainty in parameter estimation and model prediction. *Global Biogeochemical Cycles*, **20**, GB2007.
Xu X, Shi Z, Li D, Zhou X, Sherry R A, Luo Y. 2015. Plant community structure regulates responses of prairie soil respiration to decadal experimental warming. *Global Change Biology*, **21**, 3846–3853.
Yang Y, Dou Y, Wang B, Xue Z, Wang Y, An S, Chang S X. 2023. Deciphering factors driving soil microbial life-history strategies in restored grasslands. *iMeta*, **2**, e66.
Yang Y, Li T, Wang Y, Dou Y, Cheng H, Liu L, An S. 2021. Linkage between soil ectoenzyme stoichiometry ratios and microbial diversity following the conversion of cropland into grassland. *Agriculture Ecosystems and Environment*, **314**, 107418.
Yu P, Tang X, Zhang A, Fan G, Liu S. 2019. Responses of soil specific enzyme activities to short-term land use conversions in a salt-affected region, northeastern China. *Science of the Total Environment*, **687**, 939–945.
Yu Z, Zhang C, Liu X, Lei J, Zhang Q, Yuan Z, Peng C, Koerner S E, Xu J, Guo L. 2024. Responses of C:N:P stoichiometric correlations among plants, soils and microorganisms to warming: A meta-analysis. *Science of the Total Environment*, **912**, 168827.
Zhang H, Zhou Z. 2018. Recalcitrant carbon controls the magnitude of soil organic matter mineralization in temperate forests of northern China. *Forest Ecosystems*, **5**, 17.
Zhang Q, Qin W, Feng J, Li X, Zhang Z, He J, Schimel J P, Zhu B. 2023. Whole-soil-profile warming does not change microbial carbon use efficiency in surface and deep soils. *Proceedings of the National Academy of Sciences of the United States of America*, **120**, e2302190120.
Zhang Z, Hu L, Liu Y, Guo Y, Tang S, Ren J. 2025. Land use shapes the microbial community structure by altering soil aggregates and dissolved organic matter components. *Journal of Integrative Agriculture*, **24**, 827–844.

Executive Editor-in-Chief Jinshui Wu
Managing Editor Lujuan Sun